

## Electron-hole pairing and anomalous properties of layered high- $T_c$ compounds

K. B. Efetov

*Max-Planck-Institut für Festkörperforschung, Heisenbergstrasse 1,  
D-7000 Stuttgart 80, Federal Republic of Germany*

(Received 29 August 1990; revised manuscript received 27 November 1990)

Band-structure pictures for layered high- $T_c$  materials available in the literature show that, besides the dispersive broad band responsible for metallic properties, there are at least two additional bands having minima and maxima near the Fermi surface. These additional bands belong to different planes (for example, CuO planes and BiO planes in  $\text{Bi}_2\text{Sr}_2\text{CaCu}_2\text{O}_8$ ) or to planes and chains (in  $\text{YBa}_2\text{Cu}_3\text{O}_7$ ). Provided the Coulomb repulsion is not very weak, pairing of electrons and holes belonging to these additional bands in different planes or planes and chains is possible. It is shown that, if this possibility is realized, a transition in the additional bands into a state of an excitonic dielectric occurs. The spin of an electron-hole pair can be both 0 and 1. Due to the fact that the electron and the hole of the pair belong to different planes, there are no charge- or spin-density waves. This excitonic insulator can serve as a polarizing substance and give a strong attraction between electrons of the metallic band even if the bare interaction is repulsive. It is also shown that some interesting gapless excitations exist. Provided there are impurities in the system that scatter from plane to plane, these excitations are coupled to the electrons of the metallic band. This effective interaction can be described in terms of an effective mode  $P(\omega)$  with  $\text{Im}P(\omega) \sim -\text{sgn}\omega$ . As a result, one can obtain such properties of the normal state as a linear dependence of the resistivity on temperature, linear dependence of the density of states on energy, constant background in the Raman-scattering intensity, large nuclear relaxation rate, etc., which are very well known from experiments.

### I. INTRODUCTION

Since the discovery of the high- $T_c$  superconductivity,<sup>1</sup> many theoretical models have been proposed in order to explain this phenomenon. The CuO layered compounds are interesting not only due to high-transition temperatures, but the normal properties are also unusual. Properties such as the linear dependence of the resistivity on the temperature,<sup>2</sup> the linear tunneling conductivity as a function of voltage,<sup>3</sup> almost frequency- and temperature-independent backgrounds in the Raman-scattering intensity,<sup>4</sup> constant thermal conductivity,<sup>5</sup> and a very large nuclear relaxation<sup>6</sup> time are qualitatively the same in all CuO-based high- $T_c$  compounds. It is quite reasonable to expect that this anomalous behavior in the normal state and the large values of the superconductivity transition temperature have the same origin.

In many theoretical works the anomalous properties of the oxide compounds such as the high superconducting temperature and the properties of the normal state mentioned above were attributed to the existence of localized magnetic moments or to an interaction with other magnetic objects. These ideas have the natural basis because the parent compounds are antiferromagnetic. Doping destroys the antiferromagnetic order which must lead, according to Ref. 7, to a spin liquid, and then the superconductivity can be obtained. However, until now, attempts to construct a quantitative theory following these ideas, which would give the superconductivity and, at the same time, describe the properties of the normal state, are not very successful. Besides, it is not evident that the

superconductivity is due to magnetic interactions. The highest-transition temperatures are observed in such materials as  $\text{Bi}_2\text{Sr}_2\text{CaCu}_2\text{O}_8$ ,  $\text{Tl}_2\text{Ba}_2\text{Ca}_2\text{Cu}_3\text{O}_{10}$ , and  $\text{YBa}_2\text{Cu}_3\text{O}_7$ , which are metals in the normal state. The existence of localized moments in these materials is not obvious. For example, the authors of the work<sup>8</sup> where the neutron-scattering study of polycrystalline  $\text{YBa}_2\text{Cu}_3\text{O}_7$  was carried out conclude that the Cu atoms have essentially no magnetic moment. The study of crystals  $\text{YBa}_2\text{Cu}_3\text{O}_{6+x}$ , with  $x=0.45$  and  $x=0.5$  is presented in Ref. 9. Although there are clear intensity peaks in the low-energy region for  $x=0.45$ , these peaks become much smoother for  $x=0.5$ . Only in the region of higher energies do the peaks become more pronounced. The question about  $\text{YBa}_2\text{Cu}_3\text{O}_{6+x}$  with  $x$  close to unity cannot be solved in this way because, although not too much is seen for lower energies, the scattering peaks, in principle, could exist at very high energies. Such a situation would correspond to the picture of localized moments fluctuating very fast in time. At the same time, independent of the question of whether the localized moments exist or not, their importance for the superconductivity is not clear. Due to all these problems, an attempt to construct a theory for describing the superconducting and normal properties of the highly doped compounds based on non-magnetic mechanisms seems to be motivated.

When using conventional phonon mechanisms of attraction between electrons, one encounters difficulties related, for example, to the necessity of the explanation of the absence of the isotope effect. The possibility of obtaining high-transition temperatures is also not evident.

Besides, the anomalous properties of the normal state mentioned above do not follow from phonon models. Of course, an electron-phonon interaction can result in a linear temperature dependence of the resistivity for temperatures exceeding the Debye frequency. However, the linear dependence was observed in  $\text{Bi}_2\text{Sr}_2\text{CuO}_6$  already starting from 20 K. The other anomalous properties also do not follow from electron-phonon models.

I want to present in this article an attempt to obtain all the important properties of the high- $T_c$  materials starting from some peculiar features of the band structure. In the highly doped limit, the materials show metallic properties and the results of band-structure calculations can serve as a good starting point. The high- $T_c$  oxides  $\text{Bi}_2\text{Sr}_2\text{CaCu}_2\text{O}_8$ ,  $\text{Tl}_2\text{Ba}_2\text{Ca}_2\text{Cu}_3\text{O}_{10}$ , and  $\text{YBa}_2\text{Cu}_3\text{O}_7$  consist of  $\text{CuO}_2$  metallic layers. These metallic layers are separated by layers of Bi-O or Tl-O or by chains of CuO. The  $\text{CuO}_2$  layers have a dispersive band which determines metallic properties of the compounds, but also a band which has a maximum near the Fermi surface. Bi-O layers in  $\text{Bi}_2\text{Sr}_2\text{CaCu}_2\text{O}_8$  give two bands with the minima near the Fermi surface. In  $\text{Tl}_2\text{Ba}_2\text{Ca}_2\text{Cu}_3\text{O}_{10}$  these additional bands with the minima near the Fermi surface are given by Tl-O layers.

Below, a pairing of electrons and holes of the additional bands belonging to different layers or layers and chains is considered. This pairing gives rise to the state of an excitonic insulator. In spite of the dielectric pairing in the additional bands, the main dispersive band can remain metallic. The electron-hole pairs constitute an easily polarizable substance which can give an attraction between the electrons of the metallic band even if the bare interaction is repulsive. Due to the polarization, high superconducting transition temperatures can be obtained. Besides, the electron-hole pairing leads to the existence of gapless excitations. These excitations can interact with the electrons of the metallic band provided there are impurities which scatter electrons from plane to plane or magnetic impurities. The interaction of the electrons of the metallic band with the gapless excitations determines the behavior of the materials in the normal (nonsuperconducting) state. In fact, the imaginary part of the effective mode propagator obtained using the model of the electron-hole pairing is very close to the one proposed phenomenologically in Ref. 10. As a result, the properties of the normal state turn out to be similar to those obtained in Ref. 10. This gives the possibility of explaining the different experiments mentioned above.

A preliminary discussion of the proposed model has been presented elsewhere.<sup>11</sup> Now I want to give a more detailed consideration of the model and present new results concerning the anomalous properties of the normal state. The article is organized as follows.

In Sec. II the basic model is introduced. The relevance of this model to the band-structure picture is discussed. In Sec. III self-consistency equations describing the formation of the excitonic insulator are derived. Some properties of the dielectric order parameter are described. In Sec. IV a two-particle Green function is calculated. The poles of this Green function determine the spectra of excitations. In Sec. V the polarization of the excitonic insu-

lator is studied. It is shown that it can result in an attraction between electrons of the metallic band. In Sec. VI a possible mechanism of the coupling of the gapless collective excitations to the electrons of the metallic band is considered. An effective mode which describes this interaction is derived. In Sec. VII I study how the tunneling from plane to plane affects the results obtained in the previous sections. In Sec. VIII anomalous properties of the normal state are derived and a comparison with existing experiments is made. In Sec. IX a discussion of the obtained results is presented.

## II. CHOICE OF THE MODEL

In the present work, only highly doped materials like  $\text{Bi}_2\text{Sr}_2\text{CaCu}_2\text{O}_8$ ,  $\text{Tl}_2\text{Ba}_2\text{Ca}_2\text{Cu}_3\text{O}_{10}$ ,  $\text{YBa}_2\text{Cu}_3\text{O}_7$ , etc., are considered. Problems such as the study of the destruction of the antiferromagnetism by holes, structural transitions, and so on are not relevant to the subject of this work.

For all these materials a large number of electronic structure calculations have been carried out (see, for example Ref. 12). Usually the results of the band-structure calculations do not provide a good description of undoped materials because they predict a metallic behavior instead of the insulating one observed experimentally. At the same time, band-structure calculations describe metals quite well. The highly doped materials  $\text{Bi}_2\text{Sr}_2\text{CaCu}_2\text{O}_8$ ,  $\text{Tl}_2\text{Ba}_2\text{Ca}_2\text{Cu}_3\text{O}_{10}$ , and  $\text{YBa}_2\text{Cu}_3\text{O}_7$  are metals in the normal state and therefore one can start from the results of the band-structure calculations.

All the materials under consideration consist of  $\text{CuO}_2$  metallic layers separated by layers of Bi-O or Tl-O or by chains of CuO. The  $\text{CuO}_2$  layers contribute a dispersive band-structure picture crossing the Fermi energy, which provides the metallic properties of the material (let us call this band 0). One of the other  $\text{CuO}_2$  bands touches the Fermi level from below for  $\text{Bi}_2\text{Sr}_2\text{CaCu}_2\text{O}_8$  (see Ref. 12, p. 461) or is close to it for  $\text{Tl}_2\text{Ba}_2\text{CuO}_8$  (Ref. 12, p. 463) (I call it band 1). Bi-O layers for  $\text{Bi}_2\text{Sr}_2\text{CaCu}_2\text{O}_8$  give two bands which have the minima near the Fermi energy (one of them touches the Fermi energy, the other is 0.2 eV below  $E_F$ ). Tl-O layers in  $\text{Tl}_2\text{Ba}_2\text{CuO}_7$  also give a curve with the minimum near the Fermi level (band 2). The situation in  $\text{YBa}_2\text{Cu}_3\text{O}_7$  is a little bit more complicated. However, one can see at the point  $\Gamma$  (Ref. 13) the minimum of the band corresponding to chains. This band is denoted by 1 in Ref. 13. The position of this minimum is below the Fermi energy but not far from it. Some parts of another band are above the Fermi energy.

Now let us formulate the common feature of the band-structure pictures of the materials involved which will be used below: One dispersive (broad) band crossing the Fermi energy and at least two additional bands near the Fermi energy exist. These two additional bands belong to different layers or layers and chains. The only important property of these additional bands is that there are some parts of these bands near the Fermi surface and not all these parts are simultaneously above or below it.

A system with such a band-structure picture can be very unstable against the formation of a dielectric gap in

bands 1 and 2 which corresponds to the pairing of electrons and holes from different planes (or planes and chains for  $\text{YBa}_2\text{Cu}_3\text{O}_7$ ). The possibility of this instability is not included in the schemes of the band-structure calculations and therefore this instability must be considered separately.

In principle, there can be more than two additional bands. For example, there are two bands close to the Fermi surface in  $\text{Bi}_2\text{Sr}_2\text{CaCu}_2\text{O}_8$  which originate from Bi-O layers and there are many of them far from the Fermi surface. However, I want to consider as simple a model as possible, and so, only a three-band model (one broad band and two additional ones) will be considered.

The Hamiltonian of the system can be written in the form

$$\begin{aligned}
 H &= H_1 + H_0 + H_{01} , \\
 H_1 &= \sum_{\alpha, j=2n+1} \int \phi_{\alpha j}^\dagger(r) \varepsilon_1(-i\nabla) \phi_{\alpha j}(r) dr \\
 &+ \sum_{\alpha, j=2n} \int \phi_{\alpha j}^\dagger(r) \varepsilon_2(-i\nabla) \phi_{\alpha j}(r) dr \\
 &+ \sum_{i, j, \alpha, \beta} \int V_{ij}(r-r') \phi_{\alpha i}^\dagger(r) \phi_{\beta j}^\dagger(r') \\
 &\quad \times \phi_{\beta j}(r') \phi_{\alpha i}(r) dr dr' , \\
 H_0 &= \sum_{\alpha, j=2n+1} \int \Phi_{\alpha j}^\dagger(r) \varepsilon_0(-i\nabla) \Phi_{\alpha j}(r) dr , \\
 H_{01} &= 2 \sum_{\alpha, \beta, i, j=2n+1} \int V_{ij}(r-r') \Phi_{\alpha j}^\dagger(r) \phi_{\beta i}^\dagger(r') \\
 &\quad \times \phi_{\beta i}(r') \Phi_{\alpha j}(r) dr dr' .
 \end{aligned} \tag{2.1}$$

In Eq. (2.1),  $i, j$  label the planes,  $\alpha, \beta$  are spin indices,  $\varepsilon_0(-i\nabla)$ ,  $\varepsilon_1(-i\nabla)$ ,  $\varepsilon_2(-i\nabla)$  stand for the energy operators for the bands labeled 0, 1, 2, and  $\Phi_i^\dagger(\Phi_i)$ ,  $\phi_i^\dagger(\phi_i)$  are the corresponding electron creation and annihilation operators. Electrons of odd layers belong to bands 0 and 1, electrons of even layers are in band 2.

I assume that the function  $\varepsilon_1(p)$  has a maximum at the point  $\mathbf{w}$ , the function  $\varepsilon_2(p)$  has the minimum at the point  $\mathbf{w}-\mathbf{Q}$ ,  $\varepsilon_0(p)$  is the broad band responsible for the metallic properties of the system. All three bands are represented in Fig. 1. The interaction  $V_{ij}(\mathbf{r}-\mathbf{r}')$  is assumed to be repulsive. This situation corresponds to the case when the Coulomb interaction is stronger than the electron-phonon one. All integrations in Eq. (2.1) are performed over the two-dimensional space. Hopping terms are not included in  $H$  in Eq. (2.1). The influence of these terms on the physical properties of the system under consideration will be discussed later.

For studying the model described by the Hamiltonian (2.1), I will use the following scheme. First, the system described by the Hamiltonian  $H_1$  is studied. It is shown that this system can be unstable against the formation of an excitonic insulator. This insulator interacts via the interaction  $H_{01}$  with electrons of the metallic band 0. As a result, the effective interaction between the electrons of band 0 can become attractive and the transition into a superconducting state in the metallic band is possible. All other effects like scattering by impurities, tunneling from

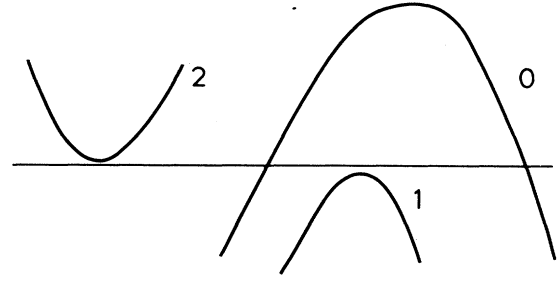


FIG. 1. Scheme of the bands. Band 2 is spatially separated from bands 0 and 1. The minimum of band 2 and the maximum of band 1 are close to the Fermi level.

plane to plane, etc., can be considered as small perturbations and taken into account in the first orders of a perturbation theory.

### III. EXCITONIC INSULATOR

In this section the system described by the Hamiltonian  $H_1$  in Eq. (2.1) is considered. It is very well known<sup>14-16</sup> that such an electron-hole system can be unstable against formation of electron-hole pairs. In order to see this instability, one should sum up the ladder diagrams represented in Fig. 2(a), where the solid lines stand for the Green functions of electrons and holes of bands 1 and 2 and dashed lines stand for the interaction  $V_{ij}(r-r')$ .

It is not difficult to see that the formation of the excitonic insulator in the system under consideration is more probable than in conventional semimetals or semiconductors, where not only the diagrams in Fig. 2(a) play a role

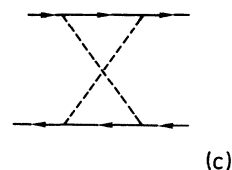
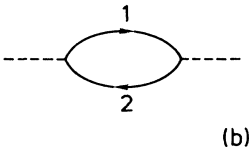
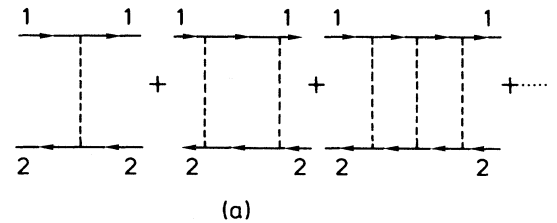


FIG. 2. The main contribution comes from (a).

but the diagrams in Fig. 2(b) are also important. Each loop in Fig. 2(b) consists of a closed fermionic line and has the opposite sign with respect to loops in Fig. 2(a). As a result, the electron-hole instability can disappear. In the case of spatially separated electrons and holes, the diagrams in Fig. 2(b) vanish and the diagrams of Fig. 2(a) give the main contribution. The diagrams in Fig. 2(c) give a smaller contribution than those in Fig. 2(a) in the case of a weak interaction and overlapping bands. In this case the instability exists for any weak interaction<sup>14</sup> because each loop in Fig. 2(a) gives a logarithmically diverging contribution. Generally speaking, it is not so and the dielectric instability only exists starting from some finite value of the interaction.

In principle, the diagrams in Fig. 2(c) can give a large contribution. Nevertheless, I will only consider the ladder diagrams in Fig. 2(a) assuming that the diagrams from Fig. 2(c) result in a renormalization of the interaction. This approach corresponds to a mean-field approximation and is quite usual when studying the excitonic dielectric state.<sup>14-16</sup> One can start calculations by writing the equations of motion corresponding to the Hamiltonian  $H_1$

$$-\frac{\partial \phi_{\alpha i}(r)}{\partial \tau} = [\varepsilon_i(-i\nabla) - \mu] \phi_{\alpha i}(r) + \sum_{j,\beta} \int V_{ij}(r-r') \phi_{\alpha i}(r) \phi_{\beta j}^\dagger(r') \phi_{\beta j}(r') dr', \quad (3.1)$$

where

$$\varepsilon_i(p) = \begin{cases} \varepsilon_1(p), & i=2n+1, \\ \varepsilon_2(p), & i=2n \end{cases},$$

$\mu$  is the chemical potential,  $\tau$  is the imaginary time.

According to the mean-field procedure, one should substitute the last term in Eq. (3.1) by the expression

$$\begin{aligned} \sum_{j,\beta} \int \kappa_{ij}^{\alpha\beta}(r-r') e^{iQr'} \phi_{\beta j}(r') dr', & \quad i=2n+1, \\ \sum_{j,\beta} \int [\kappa_{ij}^{\alpha\beta}(r-r')]^* e^{iQr'} \phi_{\beta j}(r') dr', & \quad i=2n. \end{aligned} \quad (3.2)$$

I assume from the beginning that the electron-hole pairing can occur between odd and even planes. Therefore,  $\kappa_{ij}$  can be nonzero for  $|i-j|=2n+1$  only. The effective field  $\kappa_{ij}^{\alpha\beta}$  must be found from the self-consistent condition

$$\kappa_{ij}^{\alpha\beta}(r-r') = V_{ij}(r-r') \langle T_\tau \phi_{i\alpha}(\tau, r) \phi_{j\beta}^\dagger(r, r') \rangle e^{-iQr'}, \quad (3.3)$$

$T_\tau$  is the time-ordering operator.

Using the equation of motion (3.1) with the substitution (3.2), one can write down equations for the Green functions  $G_{ij}^{\alpha\beta}(r, \tau; r', \tau')$  which are introduced in the usual way:

$$G_{ij\alpha\beta}(r, \tau; r', \tau') = -\langle T_\tau \phi_{i\alpha}(\tau, r) \phi_{j\beta}^\dagger(\tau', r') \rangle. \quad (3.4)$$

These equations have been written down<sup>11</sup> in a matrix

form. The Green functions were assumed to be matrices with respect to plane and spin indices. Now I want to write these equations considering the Green functions as matrices with respect to spin indices only. The numbers  $i, j$  of planes are present explicitly. I denote the Green function  $G_{ij}$  and  $G_{ij}^{11}$  if both  $i$  and  $j$  stand for odd planes,  $G_{ij}^{22}$  if both  $i$  and  $j$  stand for even planes,  $G_{ij}^{12}$  and  $G_{ij}^{21}$  if  $i$  and  $j$  stand for the different types of the planes. Then the equation for the Green functions in the energy and momentum representation take the form

$$\begin{aligned} [i\varepsilon - \varepsilon_1(p) + \mu] G_{ij}^{11}(\varepsilon, p) - \sum_r \kappa_{ir} G_{jr}^{21}(\varepsilon, p) &= \delta_{ij}, \\ [i\varepsilon - \varepsilon_2(p - Q) + \mu] G_{rs}^{22}(\varepsilon, p) - \sum_i \kappa_{ir}^\dagger G_{is}^{12}(\varepsilon, p) &= \delta_{rs}, \\ [i\varepsilon - \varepsilon_1(p) + \mu] G_{ir}^{12}(\varepsilon, p) - \sum_s \kappa_{is} G_{sr}^{22}(\varepsilon, p - Q) &= 0, \\ [i\varepsilon - \varepsilon_2(p - Q) + \mu] G_{ir}^{21}(\varepsilon, p - Q) - \sum_j \kappa_{jr}^\dagger G_{ji}^{11}(\varepsilon, p) &= 0. \end{aligned} \quad (3.5)$$

Equation (3.3) can be rewritten in the form

$$\kappa_{ir}(p) = -T \sum_\varepsilon \int V_{ir}(p-p') G_{ir}^{12}(\varepsilon, p') \frac{d^2 p'}{(2\pi)^2}. \quad (3.6)$$

The order parameter  $\kappa_{ir}$  in Eqs. (3.5) and (3.6) is a  $2 \times 2$  complex matrix.

One can easily exclude the functions  $G^{11}$  and  $G^{22}$  from Eqs. (3.5) and reduce these equations to one equation for  $G^{12}$

$$\begin{aligned} [i\varepsilon - \varepsilon_1(p) + \mu][i\varepsilon - \varepsilon_2(p - Q) + \mu] G_{ir}^{12}(\varepsilon, p) \\ - \sum_{j,s} \kappa_{is} \kappa_{js}^\dagger G_{jr}^{12}(\varepsilon, p) = \kappa_{ir}. \end{aligned} \quad (3.7)$$

Now let us assume that the interaction is most strong in the plane and between neighboring planes. The sign of the interaction within the plane is not important but the interaction between the neighboring planes is assumed to be repulsive.

Under this assumption, the largest values of the order parameter  $\kappa_{ir}$  are achieved when  $i$  and  $r$  denote neighboring planes. The general solution  $\kappa_{ir}$  of Eqs. (3.6) and (3.7) can be written in the form

$$\kappa_{ir} = \frac{\kappa_0}{2} \gamma_{ir} u_i [1 + \sigma_z(i-r)] u_r^\dagger, \quad (3.8)$$

where

$$\gamma_{ir} = \begin{cases} 1, & |i-r|=1, \\ 0, & \text{otherwise} \end{cases},$$

$u_i$  and  $u_r$  are arbitrary unitary matrices.

Substituting Eq. (3.8) into Eqs. (3.6) and (3.7), one can obtain the following equation for  $\kappa_0$ :

$$\kappa_0(p) = T \sum_\varepsilon \int \frac{V_{12}(p-p') \kappa_0(p')}{\{\varepsilon + i[\varepsilon_1(p) - \mu]\} \{\varepsilon + i[\varepsilon_2(p - Q) - \mu]\} + \kappa_0^2(p')} \frac{d^2 p'}{(2\pi)^2}, \quad (3.9)$$

where  $V_{12}$  is the interaction between neighboring planes.

Equation (3.9) has the trivial solution  $\kappa_0=0$ . However, a nontrivial solution can also exist provided  $V_{12}$  is not very weak and essential parts of the  $\varepsilon_1(p)$  and  $\varepsilon_2(p-Q)$  are not too far from the Fermi energy. In the case of overlapping bands,<sup>14</sup>  $V_{12}$  can be even arbitrarily small.

Of course, the procedure presented above can be performed not only for the case of the two types of planes but also for a system of planes and chains like those in  $\text{YBa}_2\text{Cu}_3\text{O}_7$ . In order to calculate the transition temperature, the gap  $\kappa_0$ , and other quantities, one needs to know the explicit form of  $\varepsilon_1(p)$ ,  $\varepsilon_2(p)$ ,  $V_{12}(p)$ . The calculation of these quantities can be done only numerically and this is not the aim of the present article. To fix ideas, I want to assume only that the transition temperature and the gap are not smaller than 0.1 eV. Explicit estimates can be done, for example, in the case of two parabolas:

$$\begin{aligned}\varepsilon_1(p) - \mu &= \xi(p)(1+c) + \varepsilon_0, \\ \varepsilon_2(p-Q) - \mu &= -\xi(p)(1-c) + \varepsilon_0, \\ \xi(p) &= \frac{(p-w)^2}{2m} - b, \quad |c| < 1.\end{aligned}\quad (3.10)$$

The effective mass  $m$  and the coefficient  $c$  in Eq. (3.10) determine the masses  $m_1$  and  $m_2$  of each band

$$\begin{aligned}m^{-1} &= \frac{1}{2}(m_1^{-1} + m_2^{-1}), \\ cm^{-1} &= \frac{1}{2}(m_1^{-1} - m_2^{-1}).\end{aligned}\quad (3.11)$$

The parabolas in Eq. (3.10) are isotropic and cannot describe a system of planes and chains. However, the form of the energies  $\varepsilon_1(p)$  and  $\varepsilon_2(p)$  (3.10) is only the simplest one. All formulas obtained below can be written easily when considering each particular case.

In what follows, the temperature will be assumed to be lower than the characteristic values of the gap  $\kappa_0$  and of other energies involved. In this limit one can substitute sums over Matsubara frequencies by integrals. The calculation of integrals becomes especially simple when the Fermi energy is in the gap region. Then, for any moments  $p$ , one of the poles in the integral in Eq. (3.9) is in the upper plane of complex  $\varepsilon$  and the other is in the lower one. (The gap in the spectrum can already exist in the bare spectrum but can also appear due to nonzero values of  $\kappa_0$ .) Below I consider only this case because this simplifies calculations. At the same time, no important features of the considered phenomenon are lost.

Calculating the integral over  $\varepsilon$  in Eq. (3.9), one can obtain

$$\kappa_0(p) = \frac{1}{8\pi^2} \int \frac{V_{12}(p-p')\kappa_0(p')}{[\xi^2(p') + \kappa_0^2(p')]^{1/2}} d^2p'. \quad (3.12)$$

Equation (3.12) is a nonlinear equation which gives the possibility to find  $\kappa_0(p)$ .

In order to find the region of parameters where nonzero solutions for  $\kappa_0$  exist, one should neglect  $\kappa_0^2(p')$  in the denominator and solve the linear integral equation for  $\kappa_0$ . For  $b > 0$ , a nonzero solution already exists for very small  $V_{12}$  (provided the Fermi level is close enough

to the intersection points). For  $b < 0$ , the gap exists in the bare spectrum. This case can be also easily considered. Introducing a new variable  $\psi(p)$ ,

$$\kappa(p) = \psi(p)\xi(p), \quad (3.13)$$

one can rewrite Eq. (3.12) in the real-space representation in the following form

$$-\frac{\nabla^2\psi(r)}{2m} - \frac{1}{2}V_{12}(r)\psi(r) = -|b|\psi(r). \quad (3.14)$$

Equation (3.17) coincides formally with the Schrödinger equation for a particle in a well.

For any  $|b|$  one can find strong enough  $V_{12}(r)$  such that nonzero solutions of Eq. (3.12) appear. If the bare gap  $|b|$  is small, then nonzero  $\kappa_0$  already appears for small  $V_{12}(r)$ . Of course, these statements are correct not only in the case when  $\varepsilon_1(p)$  and  $\varepsilon_2(p)$  are determined by Eq. (3.10), but for other cases as well.

Let us note that, in contrast to conventional excitonic insulators,<sup>14-16</sup> the electron-hole pairing considered above does not result in the appearance of static charge-density or spin-density waves. These waves can exist if one of the averages  $\langle \phi_{i\alpha}(r)\phi_{i\beta}^\dagger(r) \rangle$  is not zero and oscillates in space. In the model of spatially separated electrons and holes, these averages are zero at least in the absence of tunneling from plane to plane. Therefore, a direct observation of the spatially separated electron-hole pairing in neutron or Röntgen experiments is impossible.

Having found the solution (3.8) and (3.9) for  $\kappa_r$ , one can find the Green functions which take the simple form

$$\begin{aligned}G_{ir}^{12}(\varepsilon, p) &= \kappa_{ir} f(\varepsilon, p), \\ G_{ij}^{11}(\varepsilon, p) &= [i\varepsilon - \varepsilon_2(p-Q) + \mu] f(\varepsilon, p) \delta_{ij}, \\ G_{rs}^{22}(\varepsilon, p) &= [i\varepsilon - \varepsilon_1(p) + \mu] f(\varepsilon, p) \delta_{rs},\end{aligned}\quad (3.15)$$

where

$$f(\varepsilon, p) = \{ [i\varepsilon - \varepsilon_1(p) + \mu][i\varepsilon - \varepsilon_2(p-Q) + \mu] - \kappa_0^2 \}^{-1}.$$

The appearance of the nonzero  $\kappa_0$  leads to an additional charge transfer from plane to plane. This additional charge can be calculated using the Green function (3.15). For example, the additional charge density  $\Delta q_1$  on odd layers is equal to

$$\Delta q_1 = eT \sum_{\varepsilon} \int \{ G_{ii}^{11}(\varepsilon, p) - [i\varepsilon - \varepsilon_1(p) + \mu]^{-1} \} \frac{d^2p}{(2\pi)^2}, \quad (3.16)$$

where  $e$  is the electron charge.

Calculating the integral (3.16) with the energy spectra (3.10), one can obtain

$$\Delta q_1 = \frac{me}{2\pi} \kappa_0^2 [(b^2 + \kappa_0^2)^{1/2} + |b|]^{-1/2}. \quad (3.17)$$

The additional charge on even layers has the opposite sign.

This charge transfer can considerably change the polarization properties of the system which are very important for studying the possibility of the realization of the

high- $T_c$  superconductivity in the metallic band. Besides, due to the degeneracy of the ground-state solution (3.8) (matrices  $u$  are arbitrary), low-lying excitations exist. The presence of these excitations can be very important for understanding the properties of the normal state in the metallic band. Both these effects will be considered in the next section.

All the calculations in the present work are performed neglecting pair-breaking effects. It is well known<sup>17</sup> that normal impurities can destroy the excitonic insulator. However, this effect is important only in the limit  $\kappa_0\tau \leq 1$ , where  $\tau$  is the mean-free time. If the gap  $\kappa_0$  is of the order of magnitude 0.1–1 eV, the pair-breaking effects can become important only in the very dirty limit.

Recently, an interesting pair-breaking effect due to the Coulomb interaction with the electrons of the metallic band was considered.<sup>18</sup> Although in Ref. 18 only the Peierls instability was considered, the same consideration can be applied to the excitonic insulator. However, this mechanism of the destruction cannot be important for the large values of  $\kappa_0$  which are considered in the present article. Of course, if there are other gaps in the system which are smaller than  $\kappa_0$ , the pair-breaking effects can become very important for these additional gaps. One should remember about this possibility when considering properties of the high- $T_c$  compounds. The model under

consideration with only one dielectric gap  $\kappa_0$  is chosen in order to present the simplest picture for the layered high- $T_c$  compounds.

#### IV. COLLECTIVE EXCITATIONS

Collective excitations in conventional excitonic insulators have been considered in a number of works.<sup>19,20</sup> Due to the dependence of the interaction  $V_{ir}(p-p')$  on momenta, rather complicated excitations can exist.<sup>19</sup> Here I want to consider only the simplest excitations which can already be obtained in the case when  $V_{ir}$  does not depend on the momenta. In the language of Ref. 19, it means that only zero harmonic excitations are taken into account.

For studying collective excitations one must calculate a two-particle Green function  $K$ . For this function one can write Bethe-Salpeter equations which are represented graphically in Fig. 3. Due to the existence of the anomalous Green function, one should distinguish between the functions  $K_1$  and  $K_2$ . The function  $K_1$  describes processes when each particle finishes its propagation in the same band where it started. The function  $K_2$  corresponds to processes when both the particles change their bands. The equations for these functions take the form

$$\begin{aligned} K_{1\alpha\beta,\gamma\delta}^{ir,js}(\omega,k)[1+V_{ir}\Pi_{1\alpha\beta}^{ir}(\omega,k)] &= V_{ir}\delta_{ij}\delta_{rs}\delta_{\alpha\gamma}\delta_{\beta\delta} - V_{ir}\sum_{\alpha_1,\beta_1,t,k}\Pi_{2\alpha\alpha_1,\beta_1\beta}^{it,kr}(\omega,k)K_{2\alpha_1\beta_1,\gamma\delta}^{tk,js}, \\ K_{2\alpha\beta,\gamma\delta}^{ri,js}(\omega,k)[1+V_{ir}\Pi_{1\beta\alpha}^{ir}(-\omega,-k)] &= V_{ir}\sum_{\alpha_1,\beta_1,t,k}\Pi_{3\alpha\alpha_1,\beta_1\beta}^{rk,ti}\Pi_{1\alpha_1\beta_1,\gamma\delta}^{kt,js}(\omega,k), \end{aligned} \quad (4.1)$$

where  $\Pi_1, \Pi_2, \Pi_3$  stands for the loops

$$\begin{aligned} \Pi_{1\alpha\beta}^{ir}(\omega,k) &= \Pi_1(\omega,k) \\ &= \int G_{ii,aa}^{11} \left[ \varepsilon + \frac{\omega}{2}, p + \frac{k}{2} \right] \\ &\quad \times G_{rr,\beta\beta}^{22} \left[ \varepsilon - \frac{\omega}{2}, p - \frac{k}{2} \right] \frac{d\varepsilon d^2p}{(2\pi)^3}, \\ \Pi_{2\alpha\gamma,\beta\delta}^{it,kr}(\omega,k) &= \int G_{it,\alpha\gamma}^{12} \left[ \varepsilon + \frac{\omega}{2}, p + \frac{k}{2} \right] \\ &\quad \times G_{kr,\beta\delta}^{12} \left[ \varepsilon - \frac{\omega}{2}, p - \frac{k}{2} \right] \frac{d\varepsilon d^2p}{(2\pi)^3}, \\ \Pi_{3\alpha\gamma,\beta\delta}^{rk,ti}(\omega,k) &= \int G_{kr,\alpha\gamma}^{21} \left[ \varepsilon + \frac{\omega}{2}, p + \frac{k}{2} \right] \\ &\quad \times G_{it,\beta\delta}^{21} \left[ \varepsilon - \frac{\omega}{2}, p - \frac{k}{2} \right] \frac{d\varepsilon d^2p}{(2\pi)^3}. \end{aligned}$$

Equations (3.16) give the possibility to find the functions  $K_1$  and  $K_2$ . Poles of these functions determine the collective excitations. Equations (4.1) can be solved without any difficulties. One should first exclude the function  $K_2$ .

Then one obtains a linear equation for  $K_1$ . Taking into account the explicit form of the Green functions  $G$ , (3.15) and (3.8), one can obtain

$$\begin{aligned} K_{1\alpha\beta,\gamma\delta}^{ir,js}(\omega,k) &= V_{12}D(-\omega,-k)F^{-1}(\omega,k)\delta_{ij}\delta_{rs}\gamma_{ir} \\ &\quad \times (\delta_{\alpha\gamma}\delta_{\beta\delta} - a_{\alpha\gamma}^ri a_{\beta\delta}^ri) \\ &\quad + V_{12}D^{-1}(\omega,k)a_{\alpha\gamma}^ri a_{\beta\delta}^ri, \\ K_{2\alpha\beta,\gamma\delta}^{ri,js}(\omega,k) &= V_{12}^2\Pi_0(\omega,k)F^{-1}(\omega,k)a_{\alpha\gamma}^jr a_{\beta\delta}^is(\delta_{ij}\delta_{rs}) \\ &\quad + \delta_{rs}\delta_{i-1j} + \delta_{rs}\delta_{i+1j} \\ &\quad + \delta_{ij}\delta_{r-1s} + \delta_{ij}\delta_{r+1s}, \end{aligned} \quad (4.2)$$

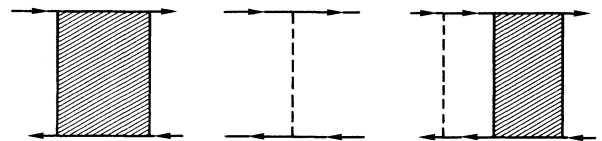


FIG. 3. Schematic Bethe-Salpeter equations which determine collective excitations.

where

$$\Pi_0(k, \omega) = \int f \left[ \varepsilon + \frac{\omega}{2}, p + \frac{k}{2} \right] \times f \left[ \varepsilon - \frac{\omega}{2}, p - \frac{k}{2} \right] \kappa_0^2 \frac{d\varepsilon d^2p}{(2\pi)^3}.$$

The functions  $D(\omega, k)$  and  $F(\omega, k)$  in Eqs. (4.2) are equal to

$$\begin{aligned} D(\omega, k) &= 1 + V_{12} \Pi_1(\omega, k), \\ F(\omega, k) &= D(\omega, k) D(-\omega, -k) - V_{12}^2 \Pi_0^2(\omega, k), \end{aligned} \quad (4.3)$$

and  $a_{\alpha\beta}^{ir}$  have the form

$$a_{\alpha\beta}^{ir} = \frac{1}{2} \gamma_{ir} [1 + \sigma_z(i-r)]. \quad (4.4)$$

Equations (4.2) and (4.4) are written for the special choice  $u_i = 1$  of matrices  $u_i$  in Eq. (3.8).

In order to determine the collective excitations one must solve the equations

$$D(\omega, k) = 0, \quad (4.5)$$

$$F(\omega, k) = 0. \quad (4.6)$$

Excitations determined by Eq. (4.5) have a gap. Equation (4.6) gives two types of excitations, one of them being gapless. Using the identity  $F(0, 0) = 0$  which follows from Eqs. (3.9) and (4.3) and expanding  $F(\omega, k)$  in  $\omega$  and  $k$ , one can obtain from Eq. (4.6)

$$\omega = vk. \quad (4.7)$$

The velocity  $v$  depends on the parameters describing bands 1 and 2. In the case when these bands are described by the symmetric parabolas (3.19) and (3.11), the velocity  $v$  of the excitations equals

$$v^2 = \frac{1-c^2}{2m} [b + (b^2 + \kappa_0^2)^{1/2}]. \quad (4.8)$$

Equation (4.7) describes complicated excitations which are a mixture of charge and spin excitations. The formal reason for the existence of these excitations is the degeneracy of the ground state. [The order parameter  $\kappa$  (3.8) is specified by arbitrary matrices  $u_i$ .] Equation (4.7) was derived under the assumption  $\omega, kv \ll \kappa_0$ .

The gapless excitations (4.7) can contribute to thermodynamic quantities. However, in the absence of impurities, they do not contribute essentially into kinetic coefficients. Although both the correlation functions  $K_1$  and  $K_2$  (4.2) are proportional to  $(\omega^2 - v^2 k^2)^{-1}$  the diverging contributions cancel each other when calculating, for example, the polarization loops  $\bar{P}^{11}$ ,  $\bar{P}^{12}$ ,  $\bar{P}^{21}$ , and  $\bar{P}^{22}$ , Fig. 4(b), because  $K_1$  and  $K_2$  give the diverging contributions of the opposite signs.

## V. POLARIZATION

Now let us study polarization properties of the electron-hole system. These properties are very important because, due to the polarization, the effective interaction between electrons of the metallic band 0 can become attractive even if the bare interaction is purely repulsive. The polarization properties can be described by the polarization loops  $B^{11}$ ,  $B^{22}$ ,  $B^{12}$ , and  $B^{21}$  represented in Fig. 4(a) and by the contributions of  $\bar{P}^{11}$ ,  $\bar{P}^{22}$ ,  $\bar{P}^{12}$ , and  $\bar{P}^{21}$  from Fig. 4(b). The  $B$  loops in Fig. 4(a) are equal to

$$\begin{aligned} B_{ij}^{mn} &= \int G_{ij}^{mn} \left[ \varepsilon + \frac{\omega}{2}, p + \frac{k}{2} \right] \\ &\times G_{ji}^{nm} \left[ \varepsilon - \frac{\omega}{2}, p - \frac{k}{2} \right] \frac{d\varepsilon d^2p}{(2\pi)^2}, \end{aligned} \quad (5.1)$$

where the Green functions  $G_{ij}^{mn}$  are given by Eq. (3.15). In the region  $\omega, kv \ll \kappa_0$ , the integrals (5.1) weakly depend on  $\omega$  and  $k$ . This region is most important for the effects considered below. Of course, the integrals (5.1) can be calculated for arbitrary  $\omega$  and  $k$ , but the results are cumbersome. Putting  $\omega, k$  zero in Eq. (5.1), assuming as before that the Fermi energy lies in the gap region, and calculating the integrals, one can obtain

$$\begin{aligned} B_{ij}^{11} &= B_{ij}^{22} = -B \delta_{ij}, \\ B_{ij}^{12} &= B_{ij}^{21} = \frac{B}{2} \gamma_{ij}, \end{aligned} \quad (5.2)$$

where

$$B = \frac{m}{4\pi} \left[ 1 + \frac{b}{(b^2 + \kappa_0^2)^{1/2}} \right],$$

$\gamma_{ij}$  is defined in Eq. (3.8).

Although the gapless excitations considered in the previous section do not give a singular contribution into the polarization, the loops  $\bar{P}^{11}$ ,  $\bar{P}^{22}$ ,  $\bar{P}^{12}$ , and  $\bar{P}^{21}$  Fig. 4(b) are not always small and must be taken into account too. The corresponding calculations are rather lengthy but not very difficult. As a result, one obtains, for  $\omega, kv \ll \kappa_0$ ,

$$\begin{aligned} \bar{P}_{ij}^{11} &= \bar{P}_{ij}^{22} = -\bar{P} \delta_{ij}, \\ \bar{P}_{ij}^{12} &= \bar{P}_{ij}^{21} = -\frac{\bar{P}}{2} \gamma_{ij}, \end{aligned} \quad (5.3)$$

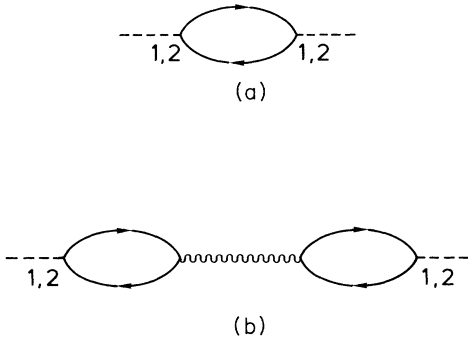


FIG. 4. Polarization loops. In (a) both the Green functions are either normal or anomalous. In (b) each loop consists of one normal and one anomalous Green function. The wavy line denotes the collective excitations given by  $K_1$  and  $K_2$ .

where

$$\bar{P} = \frac{m}{4\pi} \left[ 1 - \frac{b}{(b^2 + \kappa_0^2)^{1/2}} \right].$$

Summing both the contributions (5.2) and (5.3), one has, for the full polarization  $P_{ij}$ ,

$$P_{ij} = P_{ij}^{11} = P_{ij}^{22} = -p\delta_{ij}, \quad i \text{ and } j \text{ are both odd or even,} \quad (5.4)$$

$$P_{ij} = P_{ij}^{12} = P_{ij}^{21} = \frac{p}{2}\gamma_{ij}, \quad i \text{ and } j \text{ have different parity,}$$

where

$$p = \frac{m}{2\pi}.$$

The polarization operator  $P_{ij}$ , (5.4), can be rewritten in a convenient form in the momentum representation

$$P_{ij} = \frac{1}{2\pi} \int_0^{2\pi} e^{int} P(t) dt, \quad (5.5)$$

$$P(t) = -p(1 - \cos t), \quad n = i - j.$$

It is seen from Eq. (5.5) that  $P(0) = 0$ . At small transverse momenta  $P(t) = -(t^2 p)/2$ . Such behavior is typical for an insulator. The coefficient  $p$  determines the transverse dielectric permeability  $\epsilon_{\perp}$ . Using Eq. (5.4) one can obtain

$$\epsilon_{\perp} = 1 + e^2 m d, \quad (5.6)$$

where  $d$  is the distance between layers,  $e$  is the electron charge.

The calculation of the longitudinal dielectric permeability is more lengthy because one must make the expansion in  $k$  in the diagrams of Figs. 4(a) and 4(b). However, in the model under consideration with the spectrum (3.10), the contribution proportional  $k^2$  comes from the diagram of Fig. 4(a) only. Calculating corresponding integrals, one can obtain

$$\epsilon_{\parallel} = 1 + \frac{e^2}{3db_0} \frac{b_0 + b}{b_0 - b}, \quad (5.7)$$

where  $b_0 = (b^2 + \kappa_0^2)^{1/2}$ . Equations (5.6) and (5.7) show that the electron-hole pairing can give a considerable contribution to the static dielectric permeability. As a result, this permeability, especially the parallel one, can become much greater than unity. Of course, when studying the electromagnetic response, one should take into account the frequency-dependent contribution of the metallic band too. But this contribution can be easily separated from the contribution of the electron-hole state which depends weakly on the frequency over a wide range of the frequencies.

The electron-hole polarization gives not only the contribution to the dielectric permeability, but also changes the interaction between electrons of the metallic band, which can become attractive even if the bare interaction is repulsive. Let us consider the effective interaction in the region  $\omega, kv \ll \kappa_0$  and calculate it in the random-phase approximation (RPA). The corresponding chain diagrams are represented in Fig. 5. In the considered re-

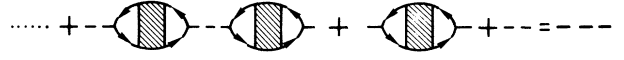


FIG. 5. The random-phase approximation for the effective interaction. Each loop  $P_{ij}$  is equal to the sum of the contributions of Figs. 4(a) and 4(b).

gion of frequencies and momenta, the bare interaction can be considered as a constant. I assume that the screening of the Coulomb interaction by the electrons of the metallic band has been taken into account and the interaction  $\tilde{V}_{ij}$  between planes already includes the contribution of the metallic band.

The equation for the effective interaction  $V_{ij}^{\text{eff}}$  takes the form

$$V_{ij}^{\text{eff}} = \tilde{V}_{ij} - \sum_{m,l} \tilde{V}_{im} P_{ml} V_{lj}^{\text{eff}}, \quad (5.8)$$

where  $P_{ij}$  is determined by Eq. (5.4). Using the Fourier transformation (5.5), one can obtain, for  $V_{ij}^{\text{eff}}$ ,

$$V_{ij}^{\text{eff}} \equiv v_n P^{-1} = \frac{1}{2\pi} \int_0^{2\pi} V^{\text{eff}}(t) \cos(nt) dt, \quad (5.9)$$

$$V^{\text{eff}}(t) = \tilde{V}(t) [1 + p(1 - \cos t) \tilde{V}(t)]^{-1},$$

where  $n = i - j$ .

Equation (5.9) solves the problem of calculating the effective interaction in the region of small frequencies and momenta  $\omega, kv \ll \kappa_0$ . In order to calculate  $V_{ij}^{\text{eff}}$  in an explicit form, one should make an assumption about the interaction  $\tilde{V}_{ij}$ . Let us take  $\tilde{V}_{ij}$  in the simplest form:

$$\tilde{V}_{ij} P = \alpha \delta_{ij} + \beta \gamma_{ij}. \quad (5.10)$$

I assume that both  $\alpha$  and  $\beta$  are positive, so the bare interaction is repulsive within the plane and between the neighboring planes (CuO and BiO) and is equal to zero in other cases. Taking the Fourier transformation of Eq. (5.10) and substituting it in Eq. (5.9), one obtains

$$v_n = \frac{1}{2\pi} \int_0^{2\pi} \frac{\cos(nt)(\alpha + 2\beta \cos t) dt}{1 + (1 - \cos t)(\alpha + 2\beta \cos t)}. \quad (5.11)$$

Formally the RPA is valid for a weak interaction. However, this scheme usually gives reasonable results for strong interactions. Of course, when carrying out the calculations, one should use, in Eq. (3.9) for the dielectric gap,  $\kappa_0$  not the bare interaction  $V_{12}$  but the corresponding interaction  $V_{12}^{\text{eff}}(|i-j|=1)$  given by Eqs. (5.9) and (5.11). For a strong enough repulsive  $V_{12}^{\text{eff}}$ , the dielectric gap  $\kappa_0$  is large and Eq. (5.11) is valid in a broad region of  $\omega$  and  $k$ . The integral (5.11) can be calculated explicitly and the result can be written in the form

$$v_n = \frac{1}{2a} [(-1)^n (1 + c - a) f_n(a + c) + (1 + a + c) f_n(a - c)], \quad (5.12)$$

where

$$c = \frac{1}{2}(\gamma - 1), \quad a = \frac{1}{2}[(\gamma + 1)^2 + 2/\beta]^{1/2},$$

$$\gamma = \frac{\alpha}{2\beta}, \quad f_n(x) = (x^2 - 1)^{-1/2} [x + (x^2 - 1)^{1/2}]^{-n}.$$

The interaction  $v_n$ , (5.12), has no singularities provided  $|c+a| > 1$  and  $|a-c| > 1$ . The second inequality is fulfilled for arbitrary parameters  $\alpha$  and  $\beta$ . The first inequality is fulfilled only if

$$\delta \equiv 4\beta(1-\gamma) < 1. \quad (5.13)$$

The scheme suggested above is only valid in the region of parameters determined by the inequality (5.13). If the inequality (5.13) is not fulfilled, the effective interaction  $V_{(t)}^{\text{eff}}$  (5.9) and (5.11), can have a pole at some transversal momentum  $t$ . Such a pole means an instability which can lead to a structural transition.

It is very important that the interaction  $v_n$  is always positive for odd  $n$ . Due to this fact, increasing the bare repulsion always favors the electron-hole pairing. In order to calculate the dielectric gap  $\kappa_0$  in the frame of the self-consistent scheme, one should substitute  $V_{12}$  in Eq. (3.9) by the effective interaction  $V_{12}^{\text{eff}}$  which is always repulsive. A strong bare repulsion  $V_{12}$  gives large values of  $V_{12}^{\text{eff}}$  and provides large values of  $\kappa_0$ .

At the same time, the interaction between different CuO planes or within one plane ( $|i-j|$  even) can be attractive. When  $\delta$  approaches 1, the first term in Eq. (5.12) is negative and its absolute value grows for all even  $n$ . It means that at least not too far from the line  $\delta=1$ , the effective interaction is attractive. For  $n=0$  the region where the interaction is negative is described by the following inequality:

$$4\gamma(1+\gamma)^{-2} < \delta < 1. \quad (5.14)$$

This region exists only for  $\gamma < 1$ . If  $\gamma > 1$ , the interaction is positive for all  $n$ . For  $n=2$ , the region of attraction is even larger due to the absence of the bare repulsion between planes with  $|i-j|=2$ . One can find a picture where these regions are drawn in Ref. 11.

Having obtained the effective attraction, one can study the question about superconductivity. In a rough ap-

proximation it is possible to try to use a BCS-like theory. One can obtain high values of the transition temperature only if the effective interaction is attractive in a large region of frequencies and momenta. At the same time, all calculations presented above are valid in the region  $\omega, vk \ll \kappa_0$ . Therefore, high  $T_c$  can be achieved only if  $\kappa_0$  is large enough. If the effective attraction between different planes is stronger than within one plane, one can expect the unusual superconductivity pairing with nonzero spin.<sup>21</sup>

## VI. COUPLING OF THE GAPLESS EXCITATIONS TO THE METALLIC BAND

In Sec. IV it was shown that the poles of the two-particle Green function  $K$  can give gapless excitation with the linear spectrum. These excitations in the absence of impurities do not give a singular contribution into the effective interaction between electrons of the metallic band. However, impurities scattering from plane to plane or magnetic impurities couple the excitations to the electrons of the metallic band. As a result a very interesting property of the normal state can be obtained.

Of course, one can make calculations using the expression (4.2) for the two-particle Green function and draw diagrams describing the coupling of the function  $K$  to the electron Green function of the metallic band. A more convenient method of calculations is to derive an effective Lagrangian describing only the gapless excitations. In this approach one first integrates out the fast-electron degrees of freedom thus reducing the problem to the study of a model containing only slow degrees of freedom.

The derivation of the Lagrangian can be carried out using the Hubbard-Stratonovich identity for the partition function  $Z$ . The procedure of the derivation is now quite usual and I only mention the main steps. The partition function  $Z$  can be represented in the following form:

$$\begin{aligned} Z &= \text{Tr} \exp(-\beta H_1) \equiv \exp(-\beta H_1^{(0)}) T_\tau \exp \left[ - \int \tilde{H}_1 d\tau \right] \\ &= A^{-1} \text{Tr} \exp(-H_1^{(0)}) T_\tau \exp \left[ - \sum_{i,j} \int [\phi_i^\dagger(r,\tau) \kappa_{ij}(r,\tau) \phi_j(r,\tau) + \text{c.c.}] dr d\tau \right] \\ &\quad \times \exp \left[ - \frac{1}{V} \text{Tr} \int \sum_{i,j} \kappa_{ij}^\dagger(r,\tau) \kappa_{ij}(r,\tau) dr d\tau \right] D\kappa \\ &\equiv \int \exp(-L) D\kappa, \quad A = \int \exp \left[ - \frac{1}{V} \int \sum_{i,j} \kappa_{ij}^\dagger(r,\tau) \kappa_{ij}(r,\tau) dr d\tau \right] D\kappa. \end{aligned} \quad (6.1)$$

First, one should calculate in Eq. (6.1) the trace over the electron degrees of freedom and reduce the partition function  $Z$  to an integral over  $\kappa$ .

The integral over  $\kappa$  in Eq. (6.1) is calculated by the saddle-point method. As the first step one should find the minimum of the Lagrangian  $L$ . The condition of the minimum coincides with the self-consistency equation

(3.3). As a result, one obtains Eq. (3.8) for  $\kappa$  in the minimum. The saddle-point solution given by Eq. (3.8) is degenerate because the matrix  $u_i$  can be arbitrary. The next step is to calculate the contribution of fluctuations near the saddle point. The fluctuations which are due to fluctuations of the matrices  $u$  are gapless.

In order to write the energy functional describing these

fluctuations, one should make an expansion of  $L$  in space and time derivatives of  $u$ . Other fluctuations have a gap and they are not as interesting as the gapless ones.

Expanding the Lagrangian  $L$  in fluctuations  $\delta\kappa$ , one can obtain usual terms  $(\delta\kappa)^2$ ,  $-(\partial\delta\kappa/\partial r)^2$ . Besides, terms  $\text{Tr}(\delta\kappa_{ij}^\dagger\delta\kappa_{ij})$  can also appear which describe the coupling of the gapless excitations with the excitations having a gap. After integration over the fluctuations with the gap, one obtains the effective Lagrangian containing only squares of the derivatives of  $\kappa$ . The final Lagrangian  $L$  describing the gapless excitations only reads

$$L = \frac{m}{8\pi\kappa_0^2} \sum_{i,j} \text{Tr} \int (\dot{\kappa}_{ij}^\dagger\dot{\kappa}_{ij} + v^2\nabla\kappa_{ij}^\dagger\nabla\kappa_{ij}) dr d\tau, \quad (6.2)$$

where  $\kappa_{ij}$  and  $v$  are given by Eqs. (3.8) and (4.8), respectively.

It is not difficult to understand why the fluctuations of the matrix  $u$  do not give a singular contribution into the polarization discussed in the previous chapter. When writing the polarization loops one always gets invariant combinations of the order parameter  $\kappa$ . For example, one can have  $\text{Tr}(\kappa_{ij}^\dagger\kappa_{ij})$  or  $\text{Tr}(\kappa_{ij}^\dagger\kappa_{kj}^\dagger\kappa_{ke}\kappa_{ie}^\dagger)$ . If the neighboring matrices  $\kappa$  are taken with equal space and time coordinates, the matrices  $u$  cancel. If the space and time coordinates are different one can expand the expression in the difference of the space and time coordinates because it is assumed that the matrices  $u$  vary slowly. As a result, one obtains expressions containing only derivatives of  $u$  and therefore the contribution of small momenta and frequencies is not singular. This result does not change if a normal impurity scattering within planes is taken into consideration.

An anomalous contribution into transport properties of the system from the region of small momenta and frequencies can arise provided there is an impurity scattering from plane to plane or magnetic scattering. These two types of impurities couple the gapless excitations to the electrons of the metallic band in a more or less similar way.

The normal impurity scattering between neighboring planes (CuO and BiO, for example) seems to be more important in the high- $T_c$  oxides and only this case is considered below.

In order to describe the interaction with the impurities which scatter from plane to plane one can add to the Hamiltonian  $H$  (2.1) the additional term  $H_{\text{imp}}$ ,

$$H_{\text{imp}} = \sum_{a,i,j} \int u_{ij}(r-r_a) [\Phi_{i\alpha}^\dagger(r) + \phi_{i\alpha}^\dagger(r)] \phi_{j\alpha}(r) + \phi_{j\alpha}^\dagger(r) [\Phi_{i\alpha}(r) + \phi_{i\alpha}(r)] dr, \quad (6.3)$$

where  $a$  stands for the number of an impurity,  $i$  and  $j$  numerate neighboring planes,  $i$  being odd and  $j$  being even. Equation (6.3) describes scattering from bands 0 and 1 into band 2 and back.

The position of the impurities is assumed to be random. In order to calculate physical quantities one must average over the positions of the impurities. In principle, the average of  $u_{ij}$  can already result in hopping terms like

$$\int [\Phi_{i\alpha}^\dagger(r) + \phi_{i\alpha}^\dagger(r)] \phi_{j\alpha}(r) dr + \text{c. c.} \quad (6.4)$$

However, it was assumed (see Fig. 1) that the minima and the maxima of the different bands are separated not only in the real space but in the momentum space also. For example, the maximum of band 1 is at the distance  $Q$  from the minimum of band 2. But the term (6.4) describes coupling with equal momenta and cannot influence essentially the gapless excitations.

One can obtain interesting effects studying second-order terms in  $H_{\text{imp}}$ . The interaction of the electrons of the metallic band with the gapless excitations can be described in terms of the interaction with an effective mode  $R(\omega)$ . This effective mode can be constructed using the effective Coulomb interaction, electron Green functions, the gapless excitations and the impurities scattering from plane to plane. The structure of this mode is represented on Fig. 6. One of the Green functions in each electron loop is normal ( $G^{11}$  or  $G^{00}$ ), the other is anomalous ( $G^{12}$  or  $G^{21}$ ). The momenta of the normal Green functions can be large but essential momenta and energies of the anomalous Green functions are small. Each loop is proportional to  $\kappa_{ij}$  or  $\kappa_{ij}^\dagger$  which are taken at different times. After integration over fast-electron variables, the effective mode  $P(\omega)$  can be expressed in terms of a time correlation of the matrices  $\kappa_{ij}$  and  $\kappa_{ij}^\dagger$  taken at the same point in space. The coincidence of the space coordinates comes from the assumed short-range interaction with impurities. Using Eq. (3.6) one can obtain for the effective mode  $R(\omega)$

$$R(\omega) = -d\tilde{A}(q, p_\perp) f(\omega),$$

$$\tilde{A}(q, q_\perp) = \frac{V_{\text{eff}}^2(q_\perp)}{V_{12}^2} [g_1^2(q) + g_2^2(q) + 2\cos(q_\perp d)g_1(q)g_2(q)], \quad (6.5)$$

where

$$g_1(q) = n|u_{ij}(q)|^2 [G^{11}(q) + G^{00}(q)],$$

$$g_2(q) = n|u_{ij}(q)|^2 G^{22}(q).$$

$n$  is the three-dimensional concentration of impurities.

The correlation function  $f(\omega)$  in Eq. (6.5) has the form

$$f(\omega) = \int \langle \text{Tr}\kappa_{ij}(r, 0) \text{Tr}\kappa_{ij}^\dagger(r, \tau) \rangle e^{i\omega\tau} d\tau. \quad (6.6)$$

In Eq. (6.6) the angular brackets stand for averaging with the free-energy functional  $L$  (6.2).

The calculation of the function  $f(\omega)$  is not difficult. In

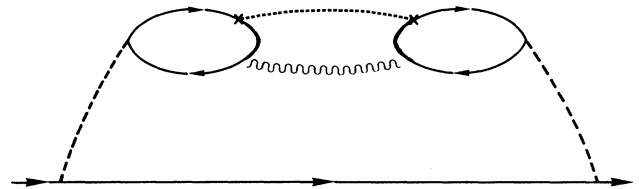


FIG. 6. Interaction with the collective excitations. The dotted line denotes the impurity correlation, the dashed line is the effective interaction. The wavy line appears after the integration over  $\kappa$  and stands for the gapless excitations.

the main approximation one should expand the matrices  $u$  in Eqs. (3.8), (6.2), and (6.6) near 1 and calculate the Gaussian integrals. As a result, one obtains

$$f(\omega) = \frac{\kappa_0^2}{\pi m} \int \frac{d^2 k}{v^2 k^2 - (\omega + i\delta)^2}. \quad (6.7)$$

Substituting Eq. (6.7) into Eq. (6.5) one can find the function  $R(\omega)$ . The imaginary part of this function can be written in the simple form

$$\begin{aligned} \text{Im}R(\omega) &= dA(q, q_\perp) \text{sgn}\omega, \\ A(q, q_\perp) &= \frac{\tilde{A}(q, q_\perp) \kappa_0^2}{mv^2}. \end{aligned} \quad (6.8)$$

The mode  $R(\omega)$  can be considered as an extra mode which can be important for studying properties of the metallic band above the superconducting temperature.

The existence of an extra mode  $\tilde{R}(\omega)$  was proposed in Ref. 10. This mode had the same form as  $R(\omega)$  (6.8) for  $\omega > T$  but was proportional to  $\omega/T$  for  $\omega < T$ . Using the hypothesis about the existence of the mode  $\tilde{R}(\omega)$ , the authors of Ref. 10 obtained such anomalous properties of the normal state as the linear resistivity, linear tunneling conductance, constant thermal conductivity, constant Raman scattering intensity, etc. Due to the opinion of the authors of Ref. 10, this mode leads to a strong attraction between electrons of the metallic band and to high superconducting temperatures.

The mode  $R(\omega)$  (6.8), as it will be shown in Sec. VIII, also gives the possibility to derive the anomalous properties of the normal state though it differs from the mode  $\tilde{R}(\omega)$  in the region  $\omega < T$ . At the same time, in the picture presented above, the main contribution to the attraction, and hence to the superconductivity, comes from the polarization which was considered in the previous section. Of course, the mode  $R(\omega)$  can also give an impurity dependent contribution to the attraction but it is not assumed to be the most essential.

## VII. TUNNELING FROM PLANE TO PLANE

Until now all the results have been obtained neglecting the possibility of the tunneling from plane to plane. Although the amplitude of the tunneling in the layered high- $T_c$  oxides is small, it is important to understand how all the results change when the possibility of the tunneling is taken into account. In order to study the influence of the tunneling, one should write an additional term  $H_t$  in the Hamiltonian

$$H_t = - \sum_{i,j} \int T_{ij}(r-r') [\phi_i^\dagger(r) \phi_j(r') + \phi_j^\dagger(r') \phi_i(r)] dr dr'. \quad (7.1)$$

In Eq. (7.1) only the terms describing the tunneling of the electrons from bands 1 and 2 are written. These terms are most interesting for studying the properties of the excitonic insulator. Of course, the tunneling of the electrons of the metallic band is very important for properties of the superconducting state. They can be described by similar terms as given by Eq. (7.1). But in the present article I want to concentrate on studying the

properties of the excitonic insulator only.

The tunneling described by the term (7.1) conserves the longitudinal momentum and does not give a direct hopping between bands 1 and 2 because they are separated in the momentum space by the large vector  $Q$ . Therefore, it is quite natural to assume that the hopping amplitude  $T_{ij}$  (7.1) has the form

$$T_{ij} = \begin{cases} \tilde{T}, & |i-j|=2, \\ 0, & \text{otherwise.} \end{cases} \quad (7.2)$$

Equation (7.2) describes hopping from CuO plane to a neighboring CuO plane for  $i, j$  odd and from BiO to BiO for  $i, j$  even.

A very important property of the electron-hole pairing considered in the present article is that there are no charge- or spin-density waves. These waves appear provided the average  $S_{\alpha\beta}$

$$S_{\alpha\beta}(r) = \langle \phi_{i\alpha}^\dagger(r) \phi_{j\beta}(r) \rangle \quad (7.3)$$

is not zero and oscillates in space with some wave vector  $q$ .

In the absence of hopping terms the oscillating part of the average (7.3) is obviously zero. One can study the effect of the hopping term (7.1) making a perturbation theory in  $\tilde{T}$ . Charge- or spin-density waves might be obtained provided some terms of the perturbation theory for  $S_{i\alpha\beta}$  (7.3) contained an odd power of  $\kappa_{ij}$ . However, this is impossible because each term of the perturbation theory contains an even number of the operators  $\phi_i, (\phi_i^\dagger)$  corresponding to band 1 and an even number corresponding to band 2.

Only direct hopping from band 1 to band 2 would give odd powers of  $\kappa_{ij}$ . Such terms can originate only from an impurity scattering. But after averaging over impurities, the terms with the odd powers  $\kappa$  vanish again.

Only large tunneling amplitudes which considerably change the band structure can give nonzero charge- or spin-density waves. In this limit the system becomes three dimensional and one can use the very well-known results.<sup>15,16</sup>

Now let us consider how the hopping term (7.1) changes the spectrum of the gapless excitations. The hopping term leads to the coupling of the order parameters  $\kappa_{ij}$  from different planes which is completely analogous to the Josephson coupling in superconductors.

Carrying out standard calculations one can obtain, in the second order in  $\tilde{T}_{ij}$ , the following additional term  $L_W$  in the Lagrangian:

$$L_W = - \frac{W^2}{4} \frac{m}{8\pi\kappa_0^2} \text{Tr}(\kappa_{i,i+1}^\dagger \kappa_{i+2,i+3} + \text{c.c.}), \quad (7.4)$$

where

$$W^2 = 2\tilde{T}^2 \left[ 1 + \frac{b}{(b^2 + \kappa_0^2)^{1/2}} \right].$$

Comparing Eq. (7.4) with the main part of the Lagrangian (6.2), one can see that the tunneling from plane to plane changes the spectrum of the gapless excitations

from that given by Eq. (4.7) to

$$\omega^2 = v^2 k^2 + \frac{W^2}{2} (1 - \cos 2k_1 d). \quad (7.5)$$

The corresponding changes must be done in Eqs. (6.7) and (6.8). As a result, one obtains, for the effective mode  $R(\omega)$  integrated over the perpendicular momentum  $k_\perp$ ,

$$\begin{aligned} \text{Im}R_0(\omega) &\equiv \frac{1}{2\pi} \int \text{Im}R(\omega) dk_\perp \\ &= -\frac{1}{A} \begin{cases} \text{sgn}\omega, & \omega > W \\ \sin^{-1}\omega/W, & \omega < W \end{cases}, \end{aligned} \quad (7.6)$$

where

$$\bar{A}(q) = \frac{d}{2\pi} \int A(q, k_\perp) dk_\perp.$$

Now the imaginary part of the effective mode  $\text{Im}R_0(\omega)$  is almost the same as the  $\text{Im}\bar{R}(\omega)$  proposed in Ref. 10. The only difference is that two different behaviors in Eq. (7.6) are separated by  $W$  and not by the temperature  $T$  as in Ref. 10. Let us emphasize that  $W$  is proportional to the tunneling amplitude from one metallic plane to another (for example, from CuO plane to CuO plane) and is very small. It can be of the order of  $T$  or even smaller. Therefore,  $\text{Im}R_0(\omega)$  can be a constant down to very low frequencies.

At the end of this chapter let us show that the solution (3.8) for  $\kappa_{ir}$  also corresponds to the minimum of the free energy for a nonzero tunneling amplitude. In order to prove this statement, let us calculate the free energy, taking for  $\kappa_{ij}$ , the following expressions:

$$\kappa_{ij}(\alpha) = \frac{\kappa_0}{2} u_i [1 + \alpha + (1 - \alpha)\sigma_z \text{sgn}(i - j)] u_j^\dagger. \quad (7.7)$$

At  $\alpha=0$ , Eq. (7.7) coincides with Eq. (3.8). One can calculate the free energy in the absence of the tunneling substituting Eq. (7.7) into Eq. (6.1) and expanding the integrals in Eq. (6.1) in  $\alpha$ . Then one can obtain for the free energy  $F(\alpha)$  in the lowest order in  $\alpha$ ,

$$F(\alpha) - F(0) = \frac{m\alpha^2\kappa_0^2}{4\pi} \left[ 1 + \frac{b}{(b^2 + \kappa_0^2)^{1/2}} \right]. \quad (7.8)$$

Equation (7.8) is written in the absence of the tunneling. It is seen that the energy  $F(\alpha)$  reaches the minimum at  $\alpha=0$ .

Now let us include the tunneling (7.1) and (7.2) and calculate the free energy in the first order in  $\tilde{T}$  and  $\alpha$ . Then one obtains the additional term  $F_T$  for the free energy per layer

$$F_T = \tilde{T} [G_{i,i+2}^{11}(r, r) + G_{i,i+2}^{22}(r, r)]. \quad (7.9)$$

For  $\alpha=0$  the Green functions in Eq. (7.9) are equal to zero. In the linear approximation one can obtain, using Eqs. (3.5) and (7.7),

$$\begin{aligned} G_{i+2,i}^{11}(\epsilon, p) &= \alpha\kappa_0^2 [i\epsilon - \epsilon_2(p - Q) + \mu] f^2(\epsilon, p), \\ G_{i+2,i}^{22}(\epsilon, p) &= \alpha\kappa_0^2 [i\epsilon - \epsilon_1(p) + \mu] f^2(\epsilon, p), \end{aligned} \quad (7.10)$$

where the function  $f(\epsilon, p)$  was introduced in Eq. (3.15).

Substituting Eq. (7.10) into Eq. (7.9) and calculating the integral over  $\epsilon$ , one can easily see that  $F_T=0$  for arbitrary  $\epsilon_1(p)$  and  $\epsilon_2(p)$ . Hence, the expansion of the free energy can start from  $\alpha^2$  only. Provided the tunneling amplitude is not very large, Eq. (3.8) for  $\kappa_{ij}$  does not change its form and one can use the results obtained in the previous chapter in a broad region of the tunneling amplitudes.

## VIII. ANOMALOUS PROPERTIES OF THE NORMAL STATE

Using the hypothesis about the existence of an extra mode  $\bar{R}(\omega)$  with some special dependence on the frequency  $\omega$ , the authors of Ref. 10 were able to obtain many well-known properties of the normal state of the high- $T_c$  materials. The mode  $R_0(\omega)$  (7.6) differs from the mode  $\bar{R}(\omega)$  because the two regimes in  $R_0(\omega)$  are separated by the coupling energy  $W$  but not by the temperature  $T$  as in Ref. 10. However, this difference is not very important for an interpretation of the experimental data.

Let us calculate the same physical quantities as those calculated in Ref. 10. The first very important quantity determining transport phenomena, photoemission, etc., is the imaginary part of the Green function. Considering the interaction of the electrons of the metallic band with the additional bosonic mode  $R_0(\omega)$ , one obtains, for the imaginary part of the self-energy  $\Sigma^R$  (Ref. 22),

$$\begin{aligned} \text{Im}\Sigma^R &= -\frac{1}{(2\pi)^4} \int dp_1 \int_{-\infty}^{\infty} d\epsilon_1 \text{Im}G^R(p_1, \epsilon_1) \\ &\quad \times \text{Im}R_0(p - p_1, \epsilon - \epsilon_1) \\ &\quad \times \left[ \tanh \frac{\epsilon_1}{2T} \right. \\ &\quad \left. + \text{coth} \frac{\epsilon - \epsilon_1}{2T} \right]. \end{aligned} \quad (8.1)$$

The function  $R_0(\omega)$  (7.6) slowly depends on the longitudinal momentum and Eq. (8.1) can be reduced immediately to a more simple one,

$$\begin{aligned} \text{Im}\Sigma^R &= \frac{N_0(0)}{2\pi^2} \int_{-\infty}^{\infty} \text{Im}R_0(\omega) \left[ \tanh \frac{\epsilon - \omega}{2T} \right. \\ &\quad \left. + \text{coth} \frac{\omega}{2T} \right] d\omega, \end{aligned} \quad (8.2)$$

where  $N_0(0)$  is the density of state in the metallic band at the Fermi surface.

For the calculation of the conductivity, one should consider a two-particle Green function. However, provided the effective mode  $R_0$  weakly depends on the longitudinal momenta, the calculation reduces to the calculation of the imaginary part of the one-particle Green function. The contribution to the resistivity coming from the scattering by the mode  $R_0$  is proportional to  $\text{Im}\Sigma^R$  (8.2). The energy  $\epsilon$  in  $\Sigma^R$  must be of the order of  $T$ .

In the limit  $W \ll T$ , the integral (8.2) is especially sim-

ple and one obtains for  $\text{Im}\Sigma^R$

$$(2\tau_R)^{-1} = -\text{Im}\Sigma^R = \frac{N_0(0)\bar{A}T}{\pi} \ln \frac{T}{W}, \quad (8.3)$$

where  $\tau_R$  is the mean time of the scattering due to the  $R$  mode,  $\bar{A}$  can be obtained from  $\bar{A}(q)$  (7.6) by averaging over all momenta  $q$  connecting points at the Fermi surface in the metallic band.

It follows from Eq. (8.3) that the resistivity  $\rho$  depends on the temperature  $T$  according to the law

$$\rho = \rho_0 + CT \ln \frac{T}{W}, \quad (8.4)$$

where  $\rho_0$  is the residual resistivity,  $C$  is a coefficient. Equation (8.4) differs from the linear law which is used to fit the experimental results.<sup>2</sup> However, it does not seem to be possible to distinguish experimentally between the linear law and the law given by Eq. (8.4). The coefficient  $C$  is proportional to the concentration of impurities scattering from plane to plane and must correlate with  $\rho_0$  which also depends on the impurity concentration.

Another quantity which was studied in Ref. 10 using the proposed hypothesis was the density of states  $N(\epsilon)$ . This quantity determines the tunneling conductance and photoemission and is connected with the Green functions as follows:

$$N(\epsilon) = -\frac{1}{\pi} \int [\text{Im}G^{00}(\epsilon, p) + \text{Im}G^{11}(\epsilon, p) + \text{Im}G^{22}(\epsilon, p)] \frac{d^2p}{(2\pi)^2}. \quad (8.5)$$

For the calculation of the imaginary parts of the Green functions one should calculate first the imaginary part of the self-energy  $\Sigma^R$  as the function of  $\epsilon$ . In the considered limit  $W \ll T$  one obtains, for arbitrary  $|\epsilon|/T$ ,

$$\sigma(\epsilon) = -\text{Im}\Sigma^R = \frac{N_0(0)\bar{A}}{2\pi} \left[ |\epsilon| + 2T \ln \frac{T}{W} \right]. \quad (8.6)$$

Of course, for  $|\epsilon| \sim T$ , Eq. (8.5) coincides with Eq. (8.3). In the region  $|\epsilon| \gg T$  one must omit the second term in Eq. (8.6) and then Eq. (8.5) is valid for arbitrary  $T/W$ .

Now let us calculate the contribution to the electron density of state coming from the imaginary part  $\text{Im}\Sigma^R(\epsilon)$ . In order to make certain estimates, let us take the spectrum of the metallic band in a quadratic form

$$\epsilon_0(p) = \frac{p^2}{2M}. \quad (8.7)$$

Calculating the first term in Eq. (8.5) one obtains the corresponding contribution  $N_0(\epsilon)$  to the density of states

$$N_0(\epsilon) = \frac{M}{2\pi} \left[ 1 - \frac{\sigma(\epsilon) + 2\tau^{-1}}{\pi\mu} \right], \quad (8.8)$$

where  $\tau$  describes scattering by normal impurities.

It is seen from Eq. (8.8) that the density of states of the metallic band has a linear  $|\epsilon|$  term with the negative sign. In Ref. 10 it was shown that the tunneling and photoemission experiments can be explained provided the den-

sity of states has a linear term in  $|\epsilon|$  with a positive coefficient. Hence, the assumption about the existence of the extra mode  $\bar{R}(\omega)$  which interacts with the electrons of one metallic band cannot explain the tunneling and photoemission experiments, at least in a simple way. However, in the model considered in the present article, an important contribution comes from bands 1 and 2, though these bands are dielectric. This contribution is due to the possibility of the scattering of the electrons by the  $R(\omega)$  mode from band 1 to band 0. Both the bands belong to the same planes and there is no reason to assume that this scattering is small. The corresponding process can also be represented by Fig. 6. The Green function of band 0 must be taken in the self-energy  $\bar{\Sigma}$  and that of bands 1 or 2 at the ends. One can see that the self-energy  $\bar{\Sigma}$  differs from  $\Sigma$  only by a coefficient  $s$  which is the ratio of the squares of the matrix elements of the scattering from band 1 to band 0 and from band 0 to band 1. Provided the inverse scattering time is smaller than the dielectric gap, one can make an expansion in  $\bar{\Sigma}(\epsilon)$ . As a result, one obtains for  $N_1(\epsilon) + N_2(\epsilon)$

$$N_1(\epsilon) + N_2(\epsilon) = \frac{s\sigma(\epsilon)}{\pi} \int \{ [G^{11}(\epsilon, p)]^2 + |G^{12}(\epsilon, p)|^2 \} \frac{d^2p}{(2\pi)^2}. \quad (8.9)$$

The calculation of the integral (8.9) is not difficult. In order to avoid complicated formulas I write the final expression putting  $c=0$ ,  $\epsilon_0=0$  in Eq. (3.10) specifying the spectrum. Then the final result for the total density of states reads

$$N(\epsilon) = N(0) + \bar{N}|\epsilon|, \quad (8.10)$$

$$\bar{N} = \frac{\bar{A}N_0(0)}{4\pi^3} \left[ \frac{m}{\kappa_0} \left[ \frac{\pi}{2} + \tan^{-1} \frac{b}{\kappa_0} \right] s - \frac{M}{\mu} \right].$$

The gap  $\kappa_0$  was assumed everywhere above to be smaller than the Fermi energy  $\mu$ . Provided  $s$  and  $m/M$  are of the order of unity, the coefficient  $\bar{N}$  is positive, which is necessary to explain the tunneling and photoemission experiments.

The thermal conductivity  $\kappa(T)$  can be calculated in the same way as the electrical one. Provided the specific heat is linear in temperature and using the Wiedemann-Franz law, one obtains the temperature-independent (or logarithmically dependent) thermal conductivity.

An interesting contribution to the optical conductivity coming from the extra mode  $R(\omega)$  is seen at frequencies which at least exceed the temperature (see the corresponding picture in Ref. 10). In this region the mode  $R(\omega)$  (7.6) coincides with the mode  $\bar{R}(\omega)$  or Ref. 10. Therefore, I can only repeat the calculation and the conclusion.

The Raman scattering is the most direct way to observe the extra mode  $R_0(\omega)$  (7.6) because it allows one to measure the imaginary part of the density-density correlation function. The mode  $R_0(\omega)$  is proportional to the density-density correlation function which can be obtained from Eq. (6.5) by dividing  $\bar{A}(q, q_\perp)$  by  $V_{\text{eff}}^2(q_\perp)$  and

putting  $q_{\perp}=0$ . Of course, one should modify  $f(\omega)$  (6.7) by introducing the tunneling  $W$  as it was done in the previous chapter. Then the Raman intensity  $I(\omega)$  takes the form

$$I(\omega) = -\bar{b}[1+n(\omega)]\text{Im}R_0(\omega), \quad (8.11)$$

where  $\bar{b}$  is a coefficient,  $R_0(\omega)$  is specified by Eq. (7.6),  $n(\omega) = [\exp(\omega/T) - 1]^{-1}$  is the Bose-Einstein factor.

In the region  $\omega > T, W$  the intensity  $I(\omega)$  (8.11) is equal to a temperature-independent constant  $\bar{A}\bar{b}$ . In the limit  $\omega \rightarrow 0$  the intensity  $I(\omega)$  is equal to

$$I(\omega) = \bar{b}\bar{A} \frac{T}{W}. \quad (8.12)$$

The crossover between these regimes depends on the ratio  $W/T$ .

A very important property of  $I(\omega)$  (8.11) is that for arbitrary temperatures  $T_1$  and  $T_2$ ,

$$\frac{I(\omega)_{T=T_1}}{I(\omega)_{T=T_2}} = \frac{1+n(\omega, T_1)}{1+n(\omega, T_2)}. \quad (8.13)$$

A flat frequency and temperature-independent mode was observed in many experiments<sup>4</sup> in the region from several hundreds inverse santimeters up to 0.5–1 eV.

Recent experiments showed<sup>23</sup> that, in some materials (YBa<sub>2</sub>Cu<sub>3</sub>O<sub>7</sub> and Bi<sub>2</sub>Sr<sub>2</sub>CaCu<sub>2</sub>O<sub>8</sub>) for certain polarizations of the incident light, the intensity remains constant even at very low frequencies which favors the hypothesis about the extra mode in the form suggested in Ref. 10. However, measurements for Bi<sub>2</sub>CaCu<sub>2</sub>O<sub>8</sub> at  $(xy)$  polarization showed that, at  $T=100$  K, the Raman intensity decreases with the frequency. In the limit  $\omega=0$  this intensity is approximately one-half of the intensity at high

frequencies. A comparison with the results of the measurements at  $T=240$  K showed that the law (8.13) fits very well. This measurement confirms the form of the extra mode  $R_0(\omega)$  (7.6) and with the help of Eq. (8.12) gives an estimate  $W \approx 200$  K. Strictly speaking, for such  $W$ , Eqs. (3.8) and (8.4) are not valid because they were obtained in the limit  $W \ll T$ . However, one can expect that the correct behavior for  $W \sim T$  does not differ too much from the linear one.

In principle, relaxation processes can modify the mode  $R_0(\omega)$ . They can be introduced by substituting  $\omega + i\gamma$  instead of  $\omega$  in Eq. (6.7). The form of the extra mode of Ref. 10 can be obtained if  $\gamma \sim T$ . If these relaxation processes contribute in a different way for different directions, the behavior of the Raman intensity can be different for different polarizations in the light. For the directions where the relaxation is not important Eqs. (8.11)–(8.13) with  $R_0(\omega)$  (7.6) can give a good description of the extra Raman mode for all frequencies. As a consequence of the relaxation, the dependence of the resistivity on the temperature can become linear without a logarithmic factor.

The gapless excitations related to the fluctuations of the matrix  $\kappa$  are a mixture of charge and spin excitations. Therefore, they can affect magnetic properties of the system. Let us calculate the magnetic susceptibility  $\chi$ . This quantity can be calculated in the same way as the density-density correlation function. One should calculate essentially the same diagrams as represented in Fig. 6 for the extra mode  $R(\omega)$ . Just as in the previous section, one can integrate first over fast-electron variables and represent the susceptibility in the form of integrals of correlation functions of  $\kappa$  taken at a different time. The result can be written in the form

$$\chi_l^{\alpha\beta}(q, \omega) = \frac{4\mu_B^2 g_l^2(q)}{V_{12}^2} \int \langle \text{Tr} \sigma^\alpha \kappa_{i,i+1}(r, \tau) \text{Tr} \sigma^\beta \kappa_{i,i+1}^\dagger(r, \tau') \rangle e^{i\omega\tau} d\tau, \quad (8.14)$$

where  $\mu_B$  is the Bohr magneton  $l=1,2$ ,  $g_l(q)$  is introduced in Eq. (6.5).

The susceptibility is written in the space representation with respect to transverse coordinates and in the momentum representation with respect to longitudinal ones. The calculation of the correlation function in Eq. (8.14) can be carried out in exactly the same way as for  $f(\omega)$  in Eq. (6.6). As a result, one can obtain for the imaginary part of the susceptibility

$$\text{Im}\chi_l(\omega) = -\frac{\mu_B^2 \kappa_0^2}{mv^2} \frac{g_l^2(q)}{V_{12}^2(q)} \begin{cases} \text{sgn}\omega, & \omega > W \\ \sin^{-1}\omega/W, & \omega < W \end{cases}. \quad (8.15)$$

The imaginary part of the susceptibility determines the nuclear relaxation rate  $T_{1l}^{-1}(T)$

$$T_{1l}^{-1}(T) \sim -\lim_{\omega \rightarrow 0} \frac{T}{\omega} \int \text{Im}\chi_l(\omega) \frac{d^2q}{(2\pi)^2}. \quad (8.16)$$

Substituting Eq. (8.15) into Eq. (8.16), one obtains for the

nuclear relaxation rate  $T_{1l}^{-1}(T)$ ,

$$T_{1l}^{-1} \sim \frac{T}{W}. \quad (8.17)$$

The coefficient of the proportionality in Eq. (8.17) is different for  $l=1$  and 2. The contribution to the nuclear relaxation rate given by Eq. (8.17) does not violate a Korringa law. At the same time,  $T_{1l}^{-1}(T)$  given by Eq. (8.17) can be 1 or 2 orders of magnitude greater than estimates based on the Fermi surface density of states because  $W$  can be several orders of magnitude smaller than the Fermi energy. In YBa<sub>2</sub>Cu<sub>3</sub>O<sub>7</sub>,  $T^{-1}(T)$  on chains is more or less linear and 2 orders of magnitude larger than the one estimated from the density of states.<sup>6</sup>  $T^{-1}(T)$  on planes is more complicated and different for Cu and O sites. The present work, and particularly Eq. (8.17), can at least explain very large values of  $T_1^{-1}(T)$ . For a detailed description of the temperature dependence one should include something else in the consideration.

## IX. DISCUSSION

An attempt to derive the most important properties of the high- $T_c$  materials starting from some peculiar features of the band-structure pictures is presented. Besides the broad metallic band, additional bands near the Fermi surface exist. These bands belong to different planes or plane and chains and have maxima and minima. In this situation, the formation of an excitonic insulator is quite possible. Electrons and holes of each electron-hole pair belong to different planes or planes and chains. Due to this pairing a dielectric gap exists in the additional bands. At the same time the main band is very broad and remains metallic. Although the dielectric order parameter can be large, no charge- or spin-density waves appear. Therefore, this dielectric order cannot be seen in neutron experiments.

The most direct way to observe this pairing is to study the spectra by photoemission and to compare them with the results of the band-structure calculations. If, according to a band picture, a band crosses the Fermi energy but this crossing is not seen experimentally it can mean that a gap appears in this band. In recent experiments for  $\text{YBa}_2\text{Cu}_3\text{O}_7$  (Ref. 24), the results of the band-structure calculations<sup>13</sup> for the main metallic bands belonging to CuO planes were confirmed very well. At the same time, no crossing of the band belonging to the chains was seen. It is in a striking contradiction with the results of the band-structure calculations and can mean the appearance of dielectric gap. Comparing the results of x-ray absorption with the results obtained using the local density approximation, the authors of Ref. 25 came to the conclusion that the experimentally observed density of states on the chains is considerably smaller than the one given by the calculations. Therefore, the appearance of dielectric gaps in additional bands cannot be unprobable.

If this dielectric substance exists, it can serve as a polarizing medium for electrons of the metallic band. Due to the layered structure of the system this polarizing medium can be considered as located between the layers. This idea, in principle, is similar to ideas proposed long ago by Little<sup>26</sup> and Ginzburg.<sup>27</sup> A strong enough polarization can give an attraction between the electrons of the metallic band.

A very strong support of the ideas presented above comes from the comparison of the results of the band-structure calculations for the high-temperature superconductor  $\text{Bi}_2\text{Sr}_2\text{CaCu}_2\text{O}_8$  and for the related compound  $\text{Bi}_2\text{Sr}_2\text{CuO}_6$  which superconducts only below 6 K.<sup>28</sup> Both the materials have almost the same broad metallic bands band 0 if describing the material in terms of the three-

band model suggested above). However, the band which has the maximum very close to the Fermi energy in  $\text{Bi}_2\text{Sr}_2\text{CaCu}_2\text{O}_8$  (band 1 in our notation) is shifted down in  $\text{Bi}_2\text{Sr}_2\text{CuO}_6$ . Besides, the minimum of band 2 in  $\text{Bi}_2\text{Sr}_2\text{CuO}_6$  is higher than in  $\text{Bi}_2\text{Sr}_2\text{CaCu}_2\text{O}_8$ . Therefore, the proposed electron-hole pairing must be much weaker in  $\text{Bi}_2\text{Sr}_2\text{CuO}_6$  than in  $\text{Bi}_2\text{Sr}_2\text{CaCu}_2\text{O}_8$ . But the polarization is efficient only for frequencies and momenta satisfying the inequality  $\omega, kv \ll \kappa_0$ . Therefore, for all small  $\kappa_0$ , the electron-hole polarization cannot give high superconducting temperatures. In my opinion, a detailed comparative study of the compounds  $\text{Bi}_2\text{Sr}_2\text{CaCu}_2\text{O}_8$  and  $\text{Bi}_2\text{Sr}_2\text{CuO}_6$  would be very useful.

Due to the dielectric pairing proposed above, some gapless excitations can exist. These excitations do not influence much the superconducting temperature. In a system without impurities these excitations also do not give an interesting contribution to quantities describing the normal state of the metallic band. However, if the probability of the impurity scattering from plane to plane is not equal to zero, the contribution of the gapless excitations becomes important. This contribution can be described in terms of the interaction of electrons of the metallic band with an effective mode  $R(\omega)$ . The imaginary part of this mode has the form  $\text{Im}R(\omega) \sim -\text{sgn}\omega$  in a broad region of frequencies  $\omega$ . This mode is very similar to the hypothetical mode proposed in Ref. 10. The main difference is that the authors of Ref. 10 assume that the mode gives a considerable contribution to the superconducting transition temperature. In the model considered in the present article, the main contribution comes from the polarization of the excitonic insulator. The fact that the Raman intensity practically does not change for the frequencies up to 0.5–1 eV means in the present approach that the dielectric gap is large (it is at least of the order 0.5–1 eV). Therefore, Eq. (5.9) for the effective interaction  $V_{\text{eff}}$  is valid in a very broad region of frequencies and momenta and high superconducting transition temperatures can be obtained.

The effective mode  $R(\omega)$  determines anomalous properties of the normal state. This question was discussed in the previous section. Of course, all quantities must be dependent on the impurity concentration. This is an important difference with the hypothesis suggested in Ref. 10.

In conclusion, an attempt to explain high superconducting transition temperature and anomalous properties of the normal state starting from a simple model was presented. To the author's opinion, this model can be considered as a candidate for the explanation of various phenomena of high- $T_c$  oxides.

<sup>1</sup>J. G. Bednorz and K. A. Müller, *Z. Phys.* **64**, 188 (1986).

<sup>2</sup>See, for example, M. Gurrvitch, and A. T. Fiory, *Phys. Rev. Lett.* **59**, 1377 (1987).

<sup>3</sup>M. Lee, A. Kapitulnik, and M. R. Beasley, in *Mechanisms of High Temperature Superconductivity*, edited by M. Kamimura

and A. Oshiyama (Springer-Verlag, Heidelberg, 1989); M. Gurrvitch *et al.*, *Phys. Rev. Lett.* **63**, 1008 (1989).

<sup>4</sup>Review of S. Sugai, *Mechanisms of High Temperature Superconductivity*, Ref. 3.

<sup>5</sup>F. Steglich, in *Materials and Mechanisms of Superconductivity*,

- edited by J. Müller and J. L. Olsen (North-Holland, Amsterdam, 1988).
- <sup>6</sup>R. E. Walstedt and W. Warren, *Mechanisms of High Temperature Superconductivity*, Ref. 3; Y. Kitaoka *et al.*, *Mechanisms of High Temperature Superconductivity*, Ref. 3; H. Yasuoka, *Mechanisms of High Temperature Superconductivity*, Ref. 3.
- <sup>7</sup>P. W. Anderson, *Science* **235**, 1196 (1987); *Phys. Rev. Lett.* **59**, 2497 (1987).
- <sup>8</sup>T. Brückel *et al.*, *Europhys. Lett.* **4**, 1198 (1987).
- <sup>9</sup>J. M. Tranquada *et al.*, *Phys. Rev. Lett.* **64**, 800 (1990).
- <sup>10</sup>C. M. Varma, P. B. Littlewood, S. Smitt-Rink, E. Abrahams, and A. E. Ruckenstein, *Phys. Rev. Lett.* **63**, 1996 (1989).
- <sup>11</sup>K. B. Efetov, *Solid State Commun.* **76**, 911 (1990).
- <sup>12</sup>W. E. Pickett, *Rev. Mod. Phys.* **61**, 433 (1989).
- <sup>13</sup>J. Yu. S. Massida, A. J. Freeman, and D. D. Koelling, *Phys. Lett. A* **122**, 203 (1987).
- <sup>14</sup>L. V. Keldysh and Yu. V. Kopayev, *Fiz. Tverd. Tela* **6**, 2791 (1964) [*Sov. Phys. Solid State* **6**, 2219 (1965)].
- <sup>15</sup>A. N. Kozlov and L. A. Maksimov, *Zh. Eksp. Teor. Fiz.* **48**, 1184 (1965) [*Sov. Phys.—JETP* **21**, 790 (1965)].
- <sup>16</sup>B. I. Halperin and T. M. Rice, in *Solid State Physics*, edited by F. Seitz, D. Turnbull, and H. Ehrenreich (Academic, New York, 1968), Vol. 21.
- <sup>17</sup>J. Zittartz, *Phys. Rev.* **164**, 575 (1967).
- <sup>18</sup>P. Hertel, J. Appel, and J. C. Swihart, *Phys. Rev. B* **39**, 6708 (1989).
- <sup>19</sup>A. N. Kozlov and L. A. Maksimov, *Zh. Eksp. Teor. Fiz.* **49**, 1284 (1965) [*Sov. Phys.—JETP* **22**, 889 (1966)].
- <sup>20</sup>D. Jerome, T. M. Rice, and W. Kohn, *Phys. Rev.* **158**, 462 (1978).
- <sup>21</sup>K. B. Efetov and A. I. Larkin, *Zh. Eksp. Teor. Fiz.* **68**, 166 (1975) [*Sov. Phys.—JETP* **41**, 760 (1975)].
- <sup>22</sup>A. A. Abrikosov, L. P. Gorkov, and I. E. Dzyaloshinskii, *Methods of Quantum Field Theory in Statistical Physics* (Prentice-Hall, New York, 1963).
- <sup>23</sup>T. Staufner, R. Hackl, and P. Müller, *Solid State Commun.* **75**, 975 (1990).
- <sup>24</sup>J. C. Campuzano *et al.*, *Phys. Rev. Lett.* **64**, 2308 (1990).
- <sup>25</sup>J. Zaanen, M. Alouani, and O. Jepsen, *Phys. Rev. B* **40**, 837 (1989).
- <sup>26</sup>W. A. Little, *Phys. Rev.* **134**, A1416 (1964).
- <sup>27</sup>V. L. Ginzburg, *Zh. Eksp. Teor. Fiz.* **67**, 2318 (1964) [*Sov. Phys.—JETP* **20**, 1549 (1964)].
- <sup>28</sup>P. A. Sterne and C. S. Wang, *J. Phys. C* **21**, L949 (1988).